Pramana – J. Phys. (2017) 88: 37
DOI 10.1007/s12043-016-1339-y

Cross over of recurrence networks to random graphs and random geometric graphs

RINKU JACOB[1], K P HARIKRISHNAN[1,*], R MISRA[2] and G AMBIKA[3]

[1]Department of Physics, The Cochin College, Cochin 682 002, India
[2]Inter-University Centre for Astronomy and Astrophysics, Ganeshkhind, Pune 411 007, India
[3]Indian Institute of Science Education and Research, Dr Homi Bhabha Road, Pashan, Pune 411 008, India
*Corresponding author. E-mail: kp_hk2002@yahoo.co.in

MS received 1 April 2016; revised 14 June 2016; accepted 20 July 2016; published online 27 January 2017

Abstract. Recurrence networks are complex networks constructed from the time series of chaotic dynamical systems where the connection between two nodes is limited by the recurrence threshold. This condition makes the topology of every recurrence network unique with the degree distribution determined by the probability density variations of the representative attractor from which it is constructed. Here we numerically investigate the properties of recurrence networks from standard low-dimensional chaotic attractors using some basic network measures and show how the recurrence networks are different from random and scale-free networks. In particular, we show that all recurrence networks can cross over to random geometric graphs by adding sufficient amount of noise to the time series and into the classical random graphs by increasing the range of interaction to the system size. We also highlight the effectiveness of a combined plot of characteristic path length and clustering coefficient in capturing the small changes in the network characteristics.

Keywords. Chaotic time series; complex networks; random graphs.

PACS Nos 05.45.−a; 05.45.Tp; 89.75.Hc

1. Introduction

Recurrence networks (RN) are complex networks constructed from the time series of dynamical systems utilizing the specific property of recurrence [1]. They are found to be especially useful for the analysis of chaotic systems because the structural and topological properties of the underlying chaotic attractor can be characterized by the statistical measures from the RN [2,3]. Over the last one decade, nonlinear time series analysis based on net theoretic measures has developed into a major field, complimentary to conventional nonlinear time series analysis, with diverse applications ranging from identifying extreme events [4] and sudden transitions in dynamical systems [5] to detecting epileptic states [6] and for studying multiphase fluid flow [7].

The construction of the RN requires time-delay embedding [8] of the scalar time series $s(1)$, $s(2)$, …, $s(N_{\mathrm{T}})$ in an M-dimensional space using a suitable time delay τ, where N_{T} is the total number of points in the time series. The procedure creates $N = N_{\mathrm{T}} - (M-1)\tau$ state vectors in the reconstructed space representing the attractor. For the choice of τ, we stick to the criterion commonly used, namely the first minimum of the autocorrelation function.

To construct the RN, every point on the attractor is considered as a node. A reference node $\imath$ is considered to be connected to another node $\jmath$ if the distance between their representative points on the reconstructed attractor is less than or equal to a recurrence threshold ϵ. The resulting complex network is the RN. If two nodes $\imath$ and $\jmath$ are connected, the $\imath\jmath$th element R_{ij} of the recurrence matrix $\mathcal{R}$ is 1 and otherwise it is 0. The adjacency matrix $\mathcal{A}$ of the RN is obtained by removing the self-loop from $\mathcal{R}$:

$$\mathcal{A} \equiv \mathcal{R} - \mathcal{I}. \tag{1}$$

Note that by construction, $\mathcal{A}$ is a binary symmetric matrix with elements 0 or 1 because the RN is unweighted and undirected.

The value of the critical threshold ϵ_{c} used for the construction of the RN depends on the size of the

attractor. To get approximately the same range of ϵ_c for different chaotic systems for comparison of the network measures, we first transform the time series to a uniform deviate so that the size of the reconstructed attractor is confined to a unit cube $[0, 1]^M$ after embedding. It is not a trivial rescaling transformation and we have already shown how important the uniform deviate transformation is in computing conventional nonlinear measures like correlation dimension D_2 [9], especially from higher-dimensional systems [10]. The critical value ϵ_c is chosen as the value of ϵ at which a giant component for the RN appears as suggested by Donges *et al* [11] and Eroglu *et al* [12].

As an example, we show the construction of RN from the standard Rössler attractor in figure 1. The left panel shows the time series and the embedded attractor with $M = 3$ and the right panel shows the RN and the degree distribution $P(k)$ vs. k which is a probability distribution of the number of nodes $n(k)$ having a degree k. The error bar in the degree distribution is the statistical error arising out of the finiteness in the number of nodes and is given by $\sqrt{n}(k)/N$ and becomes normalized as $1/N$ if $n(k) \to 0$. The colour gradient on the RN is based on the degree of nodes. We use the Gephi software (https://gephi.org/) for the graphical representation of the network.

Note that, by construction, all the RNs satisfy two important properties. Firstly, every node in a RN is connected only to nodes within a threshold value and long-range connections are absent in the RN. Hence, RNs can be considered as spatially constrained networks [13,14] analogous to random geometric graphs (RGG) which are RGs with a metric where each of the N vertices is assigned random coordinates in a box $[0, 1]^M$ and vertices only within a finite range are connected by an edge [15]. Because of the average connectivity, the degree distribution of RGG is close to a Poissonian and as the range of interaction approaches the system size, the RGG tends to the classical RG [15]. We show below that RNs are much richer in properties compared to RGG and all RNs can make a smooth transition to RGG under some limiting conditions.

Secondly, the local probability density of the invariant measure of the attractor is mapped on to the local connectivity of the RN [14]. Consequently, the local

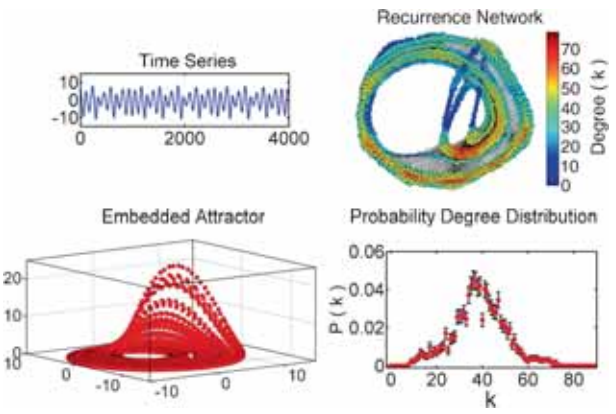

Figure 1. The construction of the RN from the time series of the standard Rössler attractor using the x-component with time step $\Delta t = 0.05$ and delay $\tau = 24$. The time series and the embedded attractor are shown in the left panel while the RN and its degree distribution are shown in the right panel.

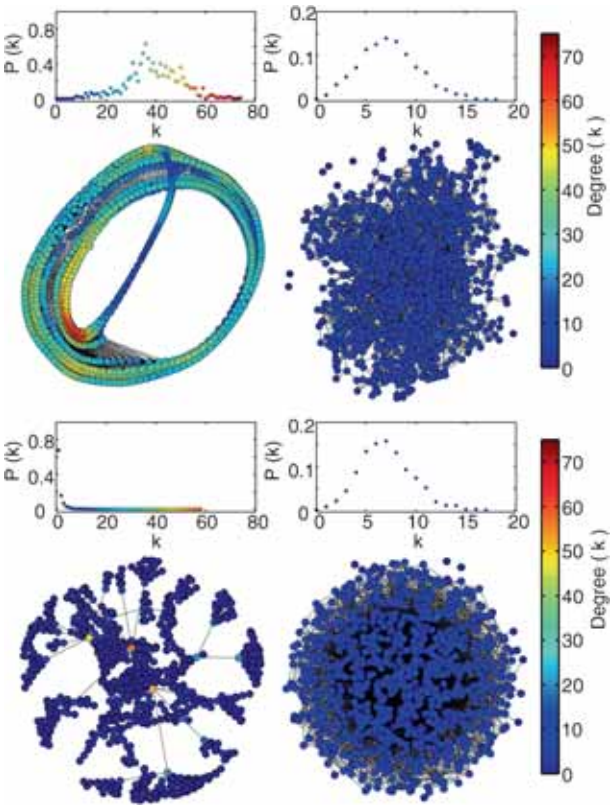

Figure 2. The networks shown in the top panel are the RNs, one computed from the time series of the standard Rössler attractor on the left and the other from random time series. The networks in the bottom panel are a synthetic SF network (on the left) with $\gamma = 2.45$ generated using the Barabasi scheme and a typical RG with connection probability $p = 0.0035$. All the networks consist of 2000 nodes. The degree distribution of each network is also shown on top of each network. The colour grading is based on the degree of nodes and is common to the network and the distribution. The RG is so chosen that its degree distribution almost exactly coincides with that of the RN from random time series. Note that the maximum value of degree ($k_{\max}$) in the RN of Rössler attractor is greater than that of the hubs in the SF network.

clustering of nodes is a manifestation of the probability density variations over the attractor [13] which in turn, is characteristic of the structure of the attractor. In this paper, we numerically show how the RNs are different from the SF and random networks in terms of the basic network measures. Our main results are given in the next section and conclusions are drawn in §3.

2. Comparison with random and scale-free networks

Two topologies of complex networks have been widely discussed in the literature for the development of theoretical ideas as well as practical applications: the random topology and the scale-free topology. The mathematical basis for the analysis of complex networks was laid many years back by Erdős and Rényi [16] using the so-called random graphs (RG). Here, there is a constant and random probability for two nodes being connected and hence for large number of nodes N, the degree distribution tends to be Poissonian.

The recent surge of interest in complex networks is due to the discovery [17,18] that the networks corresponding to many real-world interactions, be it communicative [19] or social [20], deviate from the random topology and show scale invariance. The characteristic feature of such scale-free (SF) networks is the presence of a small number of hubs or nodes with very large degree. Such networks evolve through a preferential attachment [17] of nodes and their degree distribution follows a power law $P(k) \propto k^{-\gamma}$, with the value of the scaling index γ falling between 2 and 3.

To compute the network measures, we first construct an ensemble of synthetic networks, both random and scale-free. We use the basic scheme provided in the website www.barabasilab.com for the construction of SF networks [21]. We also use two undirected and unweighted SF networks from the real world, namely, the metabolic network of yeast and the protein interaction network, for this comparative study. These are obtained from the websites: math.mist.gov/Rpozo/complex-datasets.html and www3.nd.edu/networks/resources.html. Networks with mainly $N = 2000$ or more are used for the analysis.

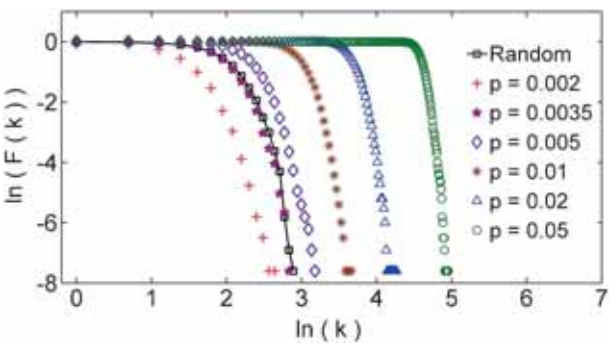

Figure 3. The cumulative degree distribution of E–R networks with different p values along with that of random RN (squares connected by solid line), which coincides with E–R network for $p = 0.0035$. In all the cases, $N = 2000$.

In figure 2, we compare the RN with networks from other classes along with their degree distributions. We choose the standard Rössler attractor as the prototype for the RN and a typical SF network with $\gamma = 2.45$. RN from a random time series is also constructed using $M = 3$ whose degree distribution is Poissonian with $\langle k \rangle \approx 7$. We show the RG with $p = 0.0035$ to make $\langle k \rangle$ equal to that of the RN.

From the figure, it is clear that the degree distribution of the RN from random time series and the RG with the given specification are almost identical. We have also computed the degree distribution of the RGG in three dimensions with the interaction range limited by the threshold $\epsilon_c = 0.1$, which coincides exactly with that of RN. Thus, the three distributions are found to be identical. However, we shall show that the classical RG deviates and is completely different from the RN and RGG in terms of the other network measures. Comparing the RN with the SF network, the difference in the degree distributions is obvious. The k values of the RN vary over a wide range determined by the local probability density variations over the attractor. Due to this correlation, the topology of the RN closely

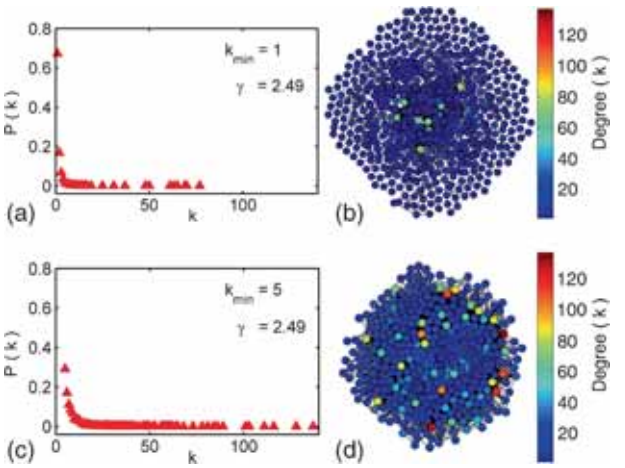

Figure 4. Comparison of two SF networks and their distributions with the same value of $\gamma = 2.49$, but having different values for k_{min}. As k_{min} increases, the range of k values increases correspondingly and nodes with much higher k values are present to maintain the same γ. In both cases, $N = 2000$.

resembles that of the embedded attractor, with nodes corresponding to regions of high probability density in the attractor having higher degree in the RN and vice versa.

To compare the degree distribution, it is more convenient to use the cumulative degree distribution which is extensively used [22] to study the trend in the distribution. It is given by

$$F(k) = \sum_{k'=k}^{k_{\max}} P(k') \tag{2}$$

plotted as a function of k. In figure 3, we plot $F(k)$ vs. k in a log–log scale for RNs from random time series along with that for RGs for p values varying from 0.002 to 0.05. The graph for RN coincides with that of E-R network (RG) with $p = 0.0035$.

In the case of SF networks, the characteristics of the network depend on two factors, the scaling index γ and the minimum value of the degree $k_{\min}$ in the network. If $k_{\min}$ is increased keeping γ fixed, the range of k values and hence $k_{\max}$ should increase correspondingly to keep γ constant. This may also change the tree structure appearance of the SF network. For example, two SF networks with identical γ and different $k_{\min}$ are compared in figure 4 along with the degree distribution. Note that the network with $k_{\min} = 5$ has a much longer range of k values and appears to have a random topology. Thus, for a complex network that may appear random, the SF property and the power law may exist for an intermediate range of k values. The characteristics of SF networks can be changed either by changing γ or by changing $k_{\min}$.

To get a comparison between different networks, we plot the cumulative degree distributions of the RNs from several standard chaotic time series with that of an E–R network, a synthetic SF network and a real-world network. The number of nodes used is 5000 for all synthetic networks. To construct the RN, the natural dimension of the attractor is used, namely, $M = 3$ for continuous systems and $M = 2$ for maps. The results are shown in figure 5. The position where $F(k)$ drops from the steady value follows a pattern in accordance with the dimension D_2 of the attractor. This position is determined by the average degree $\langle k \rangle$ which, in turn, corresponds to the average correlation sum $C_M(\epsilon_c)$ in the conventional scaling. Its value scales inversely with the dimension of the attractor for a given N [13].

We now show that this structural information and topology of the RN can be disrupted by adding random noise. If the amount of noise becomes sufficiently

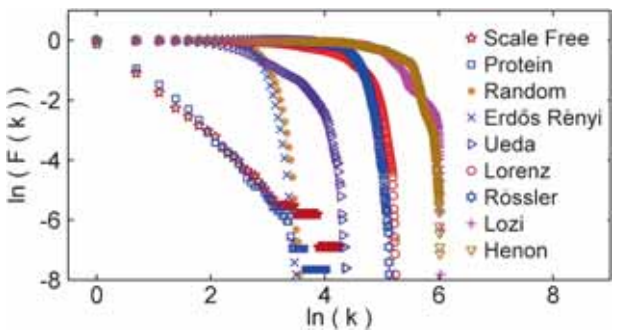

Figure 5. Comparison of the cumulative distribution of networks with different topologies with that of RNs from standard chaotic attractors, with $N = 2000$.

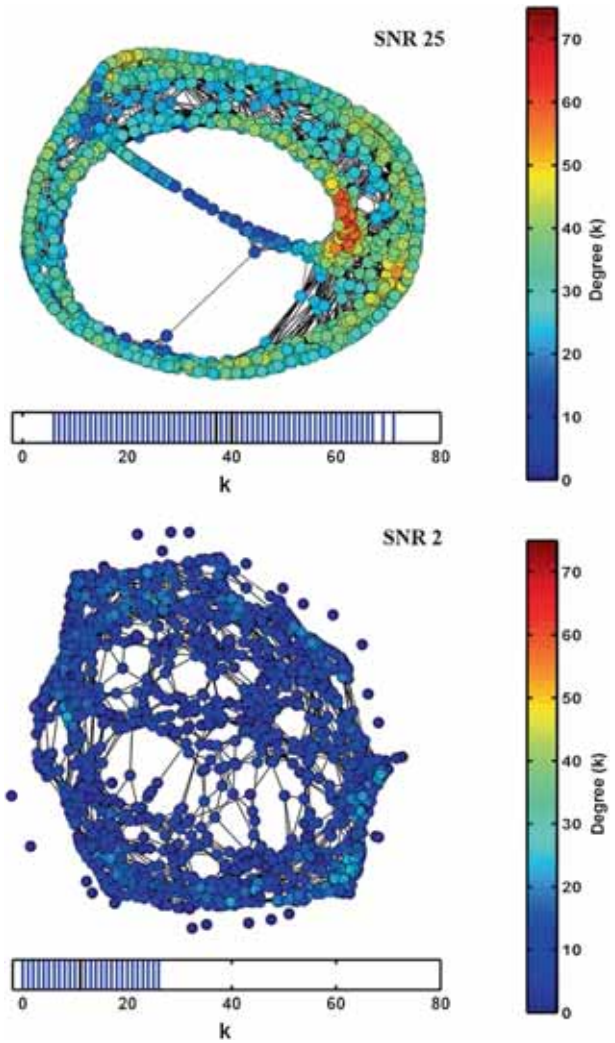

Figure 6. The influence of white noise on the topology of the RN from a chaotic attractor. The noise destroys the recurrence of the trajectory points and the RN tends towards that from random time series. The top panel shows the RN from the Rössler attractor added with 4% of noise while the bottom panel shows the same with 50% noise. The spectrum of k values for the two networks are also shown.

high, the RN loses the characteristic structural information of the attractor. To show this, we construct the RN by adding different percentages of white noise to the time series from the Rössler attractor. In figure 6, we present RNs corresponding to two different noise levels, namely, 4% (SNR 25) and 50% (SNR 2). We find that the RN preserves some information of the chaotic attractor for small and moderate amount of noise addition. As the noise level reaches 50%, the topology and the degree distribution become close to that of random time series or RGG. This is shown explicitly in figure 7 where the degree distributions of the two RNs shown in the previous figure are plotted along with that of the random time series. For clarity, the spectrum of k values are also shown below each distribution. Thus, all RNs eventually make a smooth transition to RGG as the noise level reaches 50% or more.

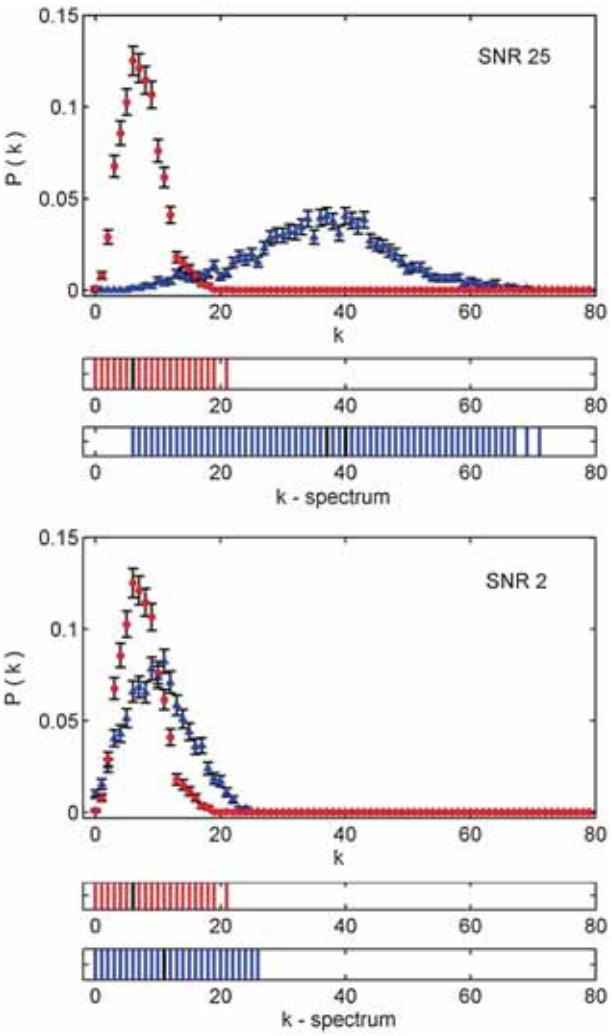

Figure 7. Comparison of the degree distribution of the two recurrence networks shown in the previous figure. As the noise level increases, the degree distribution tends towards Poissonian and the spectrum of k values shrinks. The degree distribution and the k-spectrum for the RN from the random time series are also shown in both cases.

Apart from the degree distribution, two other important measures of a complex network are the clustering coefficient (CC) and the characteristic path length (CPL). Suppose two nodes $\imath$ and $\jmath$ are connected directly to the node k. Then the CC of the node k, c_k, is the probability that the nodes $\imath$ and $\jmath$ themselves are connected. The average over all c_k in the network is the CC of the network. The CPL denoted by $\langle l \rangle$ is the average of the shortest path length l_s for all pairs of nodes $(\imath, \jmath)$ in the network. The equations for computing both CC and CPL are well known in the literature [23,24].

We use a combined CPL–CC plot to present our results of computations of CPL and CC. We find that this plot is very sensitive to small changes in the network. In figure 8, we show how random noise affects the CPL and CC values of the RN from a chaotic attractor. As expected, the values tend towards that of the RN from white noise as the noise level increases. The values of RGG coincide exactly with that of the white noise and hence are not shown.

The CPL and CC values of the RN from random time series are compared with that of E–R networks with different p values in figure 9 for $N = 2000$. Note that the RN is completely different from the RGs with respect to CPL and CC. Specifically, the position of E–R network with $p = 0.0035$, whose degree distribution

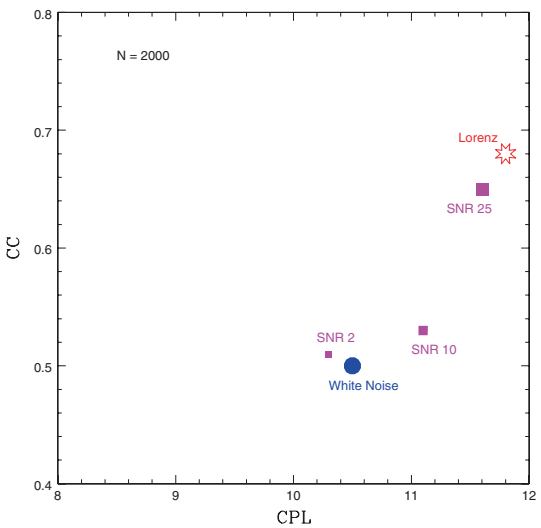

Figure 8. CPL–CC graph showing how addition of random noise affects the two measures for RN from the standard Lorenz attractor. The values for RN from pure random noise are also shown.

coincides exactly with that of RN, is much different in terms of CPL and CC. The values for $N = 5000$ for the two networks are also shown in the figure. The reason for this difference is that the nodes in the RN are connected only locally within a threshold and any long-range connections are missing in contrast to RG where the effect of the metric is absent.

We now compare the same results with the values of SF networks in figure 10. In the top panel, we show the values of different synthetic SF networks with the value of γ fixed and changing $k_{\min}$ while in the bottom panel vice versa. The values for RG with $p = 0.0035$ are also added. Though SF networks and RGs represent two

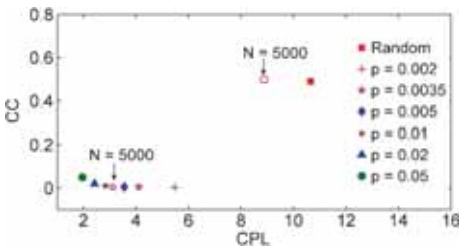

Figure 9. Comparison of CPL–CC values of random RN with that of RGs for various p values for $N = 2000$. The values for $N = 5000$ are shown (arrow mark) for RN and RG with $p = 0.0035$ whose degree distribution coincide exactly.

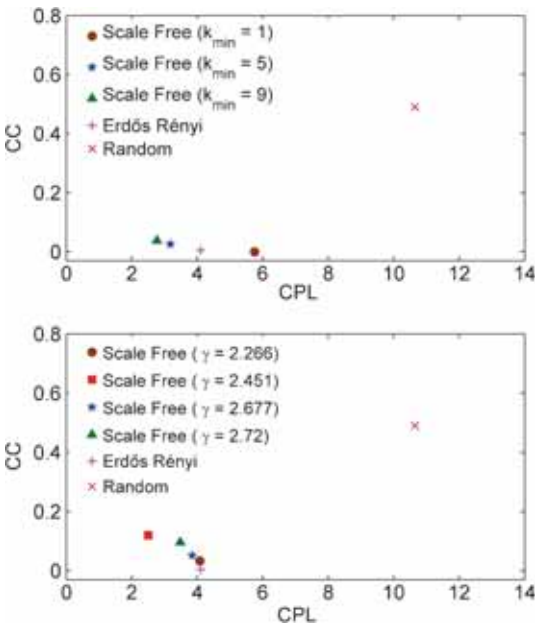

Figure 10. The top panel shows CPL–CC graphs for different synthetic SF networks with γ fixed at 2.49 and different $k_{\min}$ while the bottom panel shows the same for $k_{\min}$ fixed at 2 and different γ. In both cases, the values for random RN and the RG with $p = 0.0035$ are also included for comparison with $N = 2000$ in all the cases.

different topologies, their CPL and CC values can be made exactly the same by adjusting the parameters of both. Note that while CPL is a global measure, CC is a local measure and the combined CPL–CC plot can give both local and global characteristics of the network. Thus, combining the results from CPL–CC plot and the statistical measure of the degree distribution can provide complete information regarding the network. Two unweighted and undirected complex networks of equal number of nodes can be considered to be identical only if both the degree distribution and the CPL–CC values match exactly. In figure 11, we present the CPL–CC values of RNs from several standard chaotic attractors along with the values for two synthetic SF networks, two real-world SF networks and an RG. The results do not change much even if the number of nodes N is increased as the values saturate quickly. The figure clearly shows how the RNs are different from random and scale-free networks with respect to the two basic network measures. It is also clear that the RNs cannot display the small-world property as their CPL remains always >6.

Finally, we show that all the RNs can be changed into random topology by adjusting the threshold ϵ and they cross over to the classical RG if the range of interaction is increased to the system size. For the optimum RN (the one constructed with critical threshold ϵ_c) that characterizes the statistical properties of the chaotic attractor, the range of interaction is limited by the recurrence threshold ϵ_c. If the value of ϵ is increased, its characteristic properties are lost and it is found that all RNs smoothly cross over to RG with degree distribution tending to Poissonian and CPL $\to$ 1. This is shown in figure 12 for the RN from Lorenz and random time series. In the figure, both CC and CPL are plotted as a function of ϵ. As $\epsilon \to 1$ (the size of the attractor), all RNs make a smooth transition to RG with CPL and CC $\to$ 1 and degree distribution tending to Poissonian.

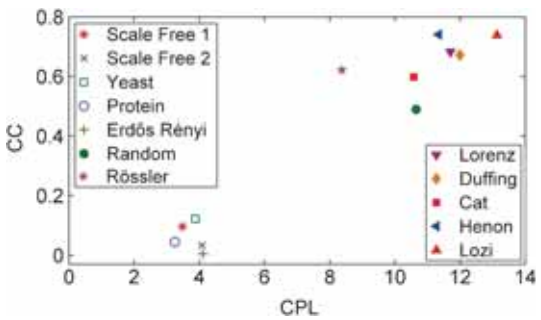

Figure 11. The CPL–CC graph for RN from several standard chaotic attractors, two-real world SF networks (protein and yeast), two synthetic SF networks and a RG.

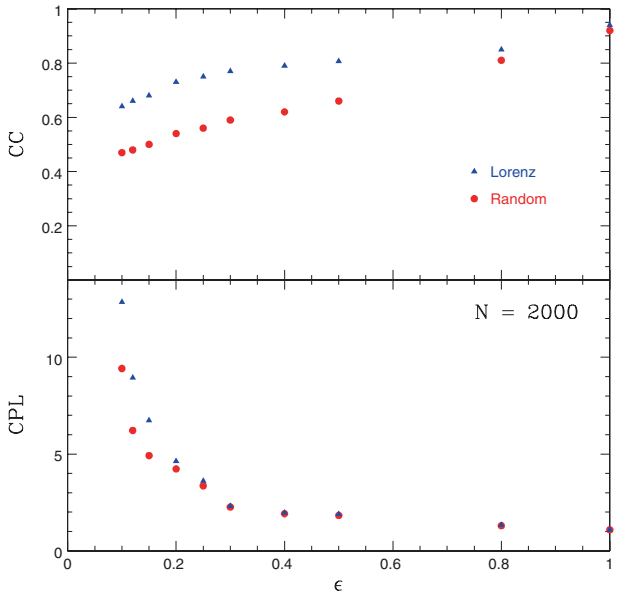

Figure 12. The figure shows the transition of RN to classical RG as the range of interaction ϵ is increased. As the value of the threshold ϵ tends to the size of the attractor, all RNs tend to classical RG with CPL and CC $\rightarrow$ 1.

It should also be mentioned here that similar results have been reported earlier in the case of planar networks as well. For example, Barthelemy [25] has proved similar results in the case of spatial networks on a plane, such as, communication and transportation networks. He has shown that the spatial effects become negligible and the networks tend to show SF property when the interaction range between the nodes is of the order of the system size or larger. He has also proposed scaling relations for this cross over for different quantities representing the network.

3. Conclusion

Networks are, in general, abstract mathematical entities that represent some complex interactions or connections in the real world. The properties of the underlying interactions are assumed to be reflected in the representative networks. From a quantitative analysis of the networks, one aims to unravel the characteristic features of the underlying structure and interactions. For example, the SF networks represent many complex interactions whose characteristic property is the scale invariance. Similarly, RNs are also representative of some natural processes, albeit, modelled by nonlinear dynamical systems. In the case of a chaotic system, the RN represents a complex distribution of trajectory points in phase space with self-similar fractal structure characteristic of a chaotic attractor.

In this paper, we compare the characteristic measures derived from the RNs of several standard chaotic attractors with that of real-world networks having either random or scale-free topology. The main motivation for this comparative study is a better understanding of the properties of RN from a complex network point of view. We find that the combined CPL–CC plot is very effective in capturing small changes in the network characteristics. Our numerical results indicate that the optimum RN is basically different from both RG and SF networks with respect to the degree distribution, CC and CPL. Since a reference node is connected only to nodes locally in the RN, the network topology closely follows that of the embedded attractor and the degree distribution reflects the probability density variations over the attractor. The absence of long-range connections also guarantees that the CPL of the optimum RNs are quite high compared to RG and SF networks. Due to the recurrence of the trajectory points as the dynamical system evolves, an increase in the number of nodes N correspondingly increase the average local connectivity $\langle k \rangle$ making the CPL to get saturated for large N. However, as the range of connectivity approaches the system size, all RNs smoothly cross over to RG with degree distribution tending to Poissonian and both CPL and CC $\rightarrow$ 1, independent of N.

We have also numerically investigated the effect of random noise contamination of the time series on the measures of the RN. As the noise level increases, the measures approach that of random time series. We have found that increasing the range of interaction between nodes and adding noise to the attractor have different effects on the RN. While the former transforms all RNs eventually to classical RG, the effect of the latter is to disrupt the local clustering, making all RNs tending to RGG.

Acknowledgements

RJ and KPH acknowledge the financial support from Science and Engineering Research Board (SERB), Govt. of India in the form of a Research Project No. SR/S2/HEP-27/2012. KPH acknowledges the computing facilities in IUCAA, Pune.

References

[1] J P Eckmann, S O Kamphorst and D Ruelle, *Europhys. Lett.* **5**, 973 (1987)

[2] R V Donner, Y Zou, J F Donges, N Marwan and J Kurths, *New J. Phys.* **12**, 033025 (2010)

[3] R V Donner, M Small, J F Donges, N Marwan, Y Zou, R Xiang and J Kurths, *Int. J. Bifurcat. Chaos* **21**, 1019 (2011)
[4] N Marwan and J Kurths, *Chaos* **25**, 097609 (2015)
[5] J F Donges, R V Donner, K Rehfeld, N Marwan, M H Trauth and J Kurths, *Nonlinear Proc. Geophys.* **18**, 545 (2011)
[6] N P Subramaniyam and J Hyttinen, *Phys. Lett. A* **378**, 3464 (2014)
[7] Z Gao, X Zhang, N Jin, R V Donner, N Marwan and J Kurths, *Europhys. Lett.* **103**, 50004 (2013)
[8] P Grassberger and I Procaccia, *Physica D* **9**, 189 (1983)
[9] K P Harikrishnan, R Misra, G Ambika and A K Kembhavi, *Physica D* **215**, 137 (2006)
[10] K P Harikrishnan, R Misra and G Ambika, *Commun. Nonlinear Sci. Numer. Simul.* **17**, 263 (2012)
[11] J F Donges, J Heitzig, R V Donner and J Kurths, *Phys. Rev. E* **85**, 046105 (2012)
[12] D Eroglu, N Marwan, S Prasad and J Kurths, *Nonlin. Processes Geophys.* **21**, 1085 (2014)
[13] Y Zou, J Heitzig, R V Donner, J F Donges, J D Farmer, R Meucci, S Euzzor, N Marwan and J Kurths, *Europhys. Lett.* **98**, 48001 (2012)
[14] R V Donner, J Heitzig, J F Donges, Y Zou, N Marwan and J Kurths, *Eur. Phys. J. B* **84**, 653 (2011)
[15] J Dall and M Christensen, *Phys. Rev. E* **66**, 016121 (2002)
[16] P Erdős and A Rényi, *Publ. Math. Inst. Hung. Acad. Sci.* **5**, 17 (1960)
[17] A L Barabasi and R Albert, *Science* **286**, 509 (1999)
[18] R Albert and A L Barabasi, *Phys. Rev. Lett.* **85**, 5234 (2000)
[19] R Albert, I Albert and G L Nakarado, *Phys. Rev. E* **69**, 025123(R) (2004)
[20] M Girvan and M E J Newman, *Proc. Nat. Acad. Sci. USA* **99**, 7821 (2002)
[21] H Jeong, Z Neda and A L Barabasi, *Europhys. Lett.* **61**, 567 (2003)
[22] M E J Newman, *Networks: An introduction* (Oxford University Press, Oxford, 2010)
[23] S H Strogatz, *Nature* **410**, 268 (2001)
[24] M E J Newman, *SIAM Rev.* **45**, 167 (2003)
[25] M Barthelemy, *Europhys. Lett.* **63**, 915 (2003)